IEEE Access
Multidisciplinary | Rapid Review | Open Access Journal

Received December 26, 2018, accepted January 13, 2019, date of publication February 4, 2019, date of current version March 20, 2019.

Digital Object Identifier 10.1109/ACCESS.2019.2895090

MILP Based Robust Short-Term Scheduling for Wind–Thermal–Hydro Power System With Pumped Hydro Energy Storage

PEI XIA, CHANGHONG DENG, YAHONG CHEN, AND WEIWEI YAO
School of Electrical Engineering and Automation, Wuhan University, Wuhan 430072, China

Corresponding author: Changhong Deng (dengch-whu@163.com)

This work was supported in part by the National Key R&D Program of China under Grant 2017YFB0902200, and in part by the State Grid Technology Program under Grant 5227221600kw.

ABSTRACT The uncertainty of the wind power generation and complex constraints of the hydropower pose challenges for the short-term scheduling of coordinated wind power, thermal power, and cascaded hydroelectric system (WTHS). In this paper, a robust security-constrained unit commitment model is established for a WTHS. The proposed model ensures the utilization of wind power and economic return from the scheduling. Conservative adjustable uncertainty sets are used to characterize the uncertainty of wind power over temporal and spatial dimensions. In this model, pumped hydro energy storage (PHES) is incorporated to cope with the wind power fluctuations. A simplified affine policy is developed for the decision making of the adjustable variables. Based on a series of linearization techniques, the proposed model is formulated as a single-level mixed-integer linear programming (MILP) problem, where the numerical tests performed on the modified IEEE 30-bus, IEEE 118-bus, and Polish 2736-bus systems verify the effectiveness of the model. The comparative analyses quantitatively evaluate the contributions of the PHES in terms of economic performance and wind power accommodation. The test results reveal that the robustness of scheduling plans is enhanced by the use of the PHES, and the proposed approach is applicable to the large-scale power systems.

INDEX TERMS Wind–thermal–hydro power system, pumped hydro energy storage, robust security-constrained unit commitment, mixed integer linear programming.

NOMENCLATURE

PARAMETERS AND CONSTANTS

N_G, N_R, N_P, N_H	Number of thermal units, wind farms, pumped hydro energy storage (PHES) stations, and hydropower plants (HPPs)
N_k, N_n	Number of units in PHES station p and HPP h
$N_{n,h}$	Number of operating zones of unit n in HPP h
N_m	Number of upstream HPPs above plant h
R_h, U_h	Segment numbers of reservoir volume and downstream flow
$C_{st,i}, C_{sd,i}$	Start-up and shut-down cost of thermal unit i
α_i^u, α_i^l	Upward and downward reserve cost coefficients of thermal unit i
$C_{pm,k,p}, C_{gn,k,p}$	Start-up cost of unit k in PHES station p for pumping and generating modes
$x_{j,t}^e$	Predicted output of wind farm j in period t
$\Delta x_{j,t}^{e,u}, \Delta x_{j,t}^{e,l}$	Upper and lower boundaries of the prediction error of wind farm j in period t
Γ_T^u, Γ_T^l	Temporal uncertainty budgets
Γ_W^u, Γ_W^l	Spatial unceirtainty budgets
β_j^u, β_j^l	Penalty cost coefficients of wind farm j
κ_h, γ_h	Penalty cost coefficient and weight factor of water flow of plant h
T	Time horizon
$\Delta T, \Delta t$	Length of the scheduling interval in hours and in seconds

The associate editor coordinating the review of this manuscript and approving it for publication was Nishad Mendis.

$T_{st,i}$, $T_{sd,i}$	Minimum start-up and shut-down time of thermal unit i
g_i^{max}, g_i^{min}	Maximum and minimum power output of thermal unit i
R_i^{up}, R_i^{dn}	Ramping up and ramping down rate of thermal unit i
$g_{z,n,h}^u$, $g_{z,n,h}^l$	Upper and lower power generation limits of zone z of unit n in plant h
q_h^{max}, q_h^{min}	Maximum and minimum downstream flows of plant h
v_h^{max} v_h^{min}	Maximum and minimum reservoir volumes of plant h
$I_{h,t}$	Water inflow of plant h in period t
τ_m	Water delay time from plant m to its direct downstream plant
$\eta_{pm,k,p}$, $\eta_{gn,k,p}$	Conversion coefficients between hydro and power of unit k in PHES station p for pumping and generating modes
$Q_p^{u,max}$, $Q_p^{u,min}$	Maximum and minimum reservoir volume of PHES station p
$Q_{p,0}^u$	Initial reservoir volume of PHES station p
$g_{pm,k,p}^{max}$, $g_{pm,k,p}^{min}$	Maximum and minimum pumping power of unit k in PHES station p
$g_{gn,k,p}^{max}$, $g_{gn,k,p}^{min}$	Maximum and minimum generating power of unit k in PHES station p
D_t	Load demand in period t
$\lambda_{r,s}$, $\lambda_{j,s}$	Quasi-steady-state generation transfer distribution factors [54] of unit r and wind farm j to the transmission line s
L_s^{max}, L_s^{max}	Transmission capacity limits of line s
I_e, I_a	Economic and accommodation indices

VARIABLES

$z_{i,t}$	Running status of thermal unit i in period t
$u_{i,t}$, $v_{i,t}$	Relaxation variables of thermal unit i in period t
$g_{i,t}$	Scheduling output of thermal unit i in period t
$\Delta g_{i,t}^u$, $\Delta g_{i,t}^l$	Upward and downward reserve capacity of thermal unit i in period t
$q_{h,t}$	Downstream flow of HPP h in period t
$s_{h,t}$	Spillage of HPP h in period t
$g_{h,t}$	Output of HPP h in period t
$g_{n,h,t}$	Output generated by unit n of HPP h in period t
$v_{h,t}$, $q_{h,t}$	Reservoir volume and downstream flow of HPP h in period t
$n_{h,t}$	Net water head of HPP h in period t
$u_{n,h,t}$	Discharge of unit n of HPP h in period t
$\Delta x_{j,t}^u$, $\Delta x_{j,t}^l$	Admissible upper and lower prediction error boundaries of wind farm j in period t
$x_{j,t}$	Actual output of wind farm j in period t
$\varsigma_{j,t}^u$, $\varsigma_{j,t}^l$	Adjustment factors of wind farm j in period t
$Q_{p,t}^u$	Upper reservoir volume of PHES station p in period t
$g_{pm,k,p,t}$, $g_{gn,k,p,t}$	Pumping and generating power of unit k of PHES station p in period t
$Q_{p,T}^u$	Reservoir volume at the end of the scheduling period
$\Delta g_{r,t}^u$, $\Delta g_{r,t}^l$	Upward and downward spinning reserve of unit r in period t
$\Delta g_{r,t}$	Regulating output of unit r in period t
$\Delta x_{j,t}$	Fluctuating power of wind farm j in period t
$y_{pm,k,p,t}$, $y_{gn,k,p,t}$	Operating status of unit k of PHES station p in period t
$u_{pm,k,p,t}$, $u_{gn,k,p,t}$	Relaxation variables of unit k of PHES station p in period t
$e_{z,n,h,t}$, $d_{\upsilon,h,t}^x$, $d_{\sigma,h,t}^y$	Binary variables
$\chi_{\sigma,\upsilon,h,t}$	Continuous variables
$\theta_{r,t}^u$, $\theta_{r,t}^l$, $J_{j,t}$, $l_{j,t}\varphi_{j,t}$	Auxiliary variables

I. INTRODUCTION

Many benefits can be achieved by the coordinated operation of multiple energy sources including wind farms, thermal power plants, and HPPs, for instance, cost effectiveness and air pollution reduction [1]. The operation efficiency and water resources utilization of HPPs can be improved if the cascaded reservoirs are applied [2]. Accordingly, optimal scheduling of the coordinated wind power, thermal power, and cascaded hydroelectric systems (WTHSs) has drawn increased attention [3].

In terms of short-term scheduling of WTHS, unit commitment (UC) is an important work to ensure the overall operation economy. Traditional UC model acquires the scheduling plan and generation level based on a deterministic power supply and load demand [4]. Mathematically, the traditional UC model is described as a mixed integer optimization problem. However, a short-term scheduling of cascaded hydroelectric system has to meet a series of nonlinear and coupling hydraulic and power generation constraints which make the problem more complicated [5]. The difficulties are mainly concentrated in the following three aspects: power generation function, operating zone restriction, and water delay time between cascaded reservoirs. Hence, approximations of the nonlinear functions of hydropower generation and tradeoffs between the accuracy and efficiency of the solution have seen significant research in the literatures [6], [7]. In recent years, mixed integer linear programming (MILP) has been increasingly used to solve the short-term scheduling problem of the cascaded hydroelectric system with efficient commercial solvers [8]–[10]. Many works have been done in this area using MILP to formulate the power generation function [11]–[13] and to the restrict operating zones [14]–[16]. Besides, Tong *et al.* [17] discuss the effects of the linearization formulation and feasibility of the solution and introduce a real number water delay. On this basis, a compact UC algorithm is developed by Guedes *et al.* [18] to reduce the dimension problem of the introduced binary variables. The above literatures have provided in-depth studies of the formulations and solutions for short-term scheduling of cascaded

hydroelectric system based on traditional UC model. However, the uncertainty inherent in wind power generation poses another challenge to the short-term scheduling of WTHS. The UC problem containing uncertainties should be modeled by considering the prediction error of wind power.

There are mainly two approaches to solve the UC problem containing uncertainties, namely, stochastic optimization and robust optimization. Stochastic optimization describes the uncertainties using probabilistic density functions or scenario trees. In the framework of stochastic optimization, an accurate probabilistic description of uncertain variables needs to be selected carefully. Nevertheless, it has increased computational requirements for large-scale problems due to the scenario generation technique as a disadvantage [19]–[21]. Robust optimization (RO) theory provides a promising scheme to address uncertainties by employing scenario sets or intervals [22]–[25]. In recent years, interval based robust security-constrained unit commitment (RSCUC) model considering transmission line constraints has received much attention. A two-stage RSCUC model has been proposed to obtain the commitment decision in the first stage and the dispatch result for the worst-case realization of uncertainty in the second stage [26]. The worst-case dispatch problem is reformulated into a MILP problem in [27]. And a very tight lower bound for the two-stage RSCUC problem is provided by a simplified model in [28]. Different worst-case definitions of RSCUC models are investigated and compared in [29].

The aforementioned researches laid a solid foundation for construction of two-stage RSCUC models. However, these models generally determine the scheduling plan and reserve capacity based on the predefined uncertainty set where wind power fluctuations can be fully compensated. With the increasing penetration of wind power in power systems, the contradiction between economy and robustness of the optimization objective is becoming more prominent, which could result in an infeasible solution for the optimization models by a predefined interval of wind power [30].

The nonanticipativity of the decisions sequence and the availability of wind power have led to increased attention to the affinely adjustable RO approach [31]. Lorca *et al*. [32] propose a multistage RSCUC model and simplify affine policies to deal with large-scale systems within a reasonable time frame. Zugno *et al*. [33] apply an affinely adjustable model for the multistage RSCUC problem in both the electricity and heat markets. These works improve the performance of the RSCUC model. However, both the two-stage and multistage RSCUC problems have a master and subproblem structures that are difficult to compute [34].

Currently, the energy storage systems are often applied in the wind power integrated systems to reduce the power fluctuation [35]–[37]. Pumped hydro energy storage (PHES) is a mature energy storage system and fast response peak-shaving plant [38] that is widely used in wind power integrated systems for long-term generation expansion [39], weekly scheduling [40], and short-term scheduling [41]. In the area of short-term scheduling, the day-ahead operations of a wind power integrated system benefits economically from the including PHES as discussed in [42]–[44]. In the work by Jiang *et al*. [45], PHES is used in a two-stage RSCUC model to cope with wind power fluctuations in the worst case scenarios that are suitable for the full accommodation of wind power. These studies provide good guidance for assessing the contribution of PHES in terms of the economic performance on the short-term scheduling for wind–thermal power systems [46], but there are only a few studies on WTHS with PHES. Shukla and Singh [47] acquire a lower operating cost by integrating PHES in WTHS. In the literature [48], PHES is designed with conventional HPP as a cascaded hydroelectric system to coordinate the short-term scheduling in wind–solar–hydro–thermal power systems. These models use stochastic optimization to tackle the uncertainty in wind power. Security of the transmission lines are not addressed, though. Besides, the modeling cascaded hydroelectric systems are simplified that may lead to inaccuracies [49].

In practice, the cascaded HPPs not only generate power but also undertake tasks such as flood control and irrigation, which limits its peak-shaving capability. However, limited attention has been paid to the operation of cascaded HPPs in current research [50]. Regulation capacity of thermal units is restricted by the ramp rate, although PHES is an effective complementary power supply when the regulation capacity of HPPs is limited, the operational feasibility and economy of wind power accommodation should be taken into account. Hence, it is valuable to investigate the potential benefits in WTHS by incorporating PHES. Furthermore, the scale of the system will be very large when wind, thermal, hydro, and PHES units are all included, which can be a complex computational task due to the increased number of units and transmission lines. In summary, the main challenges in short-term scheduling of WTHS including PHES focus on: (1) establishing a reliable UC model to handle the uncertainty of wind power and complex constraints of cascaded HPPs in a multiple energy system; (2) designing a practical and effective solution method that is computationally tractable to large-scale systems; (3) acquiring the operational feasibility and economy of wind power accommodation and quantifying the contribution of PHES. Motivated by these challenges, a novel RSCUC approach based on MILP method is proposed in this paper. In this approach, the operation as well as the regulation of cascaded HPUs is considered and described as a series of linear constraints based on a heuristic algorithm [18]. Also, uncertainty budgets of wind power over temporal and spatial dimensions are introduced and two adjustment factors are designed to ensure that the robust optimal solution is not overly conservative. Compared with previous studies, the main contributions of this paper are as follows:

(1) A short-term scheduling scheme is proposed for a WTHS including PHES based on RO. The proposed model coordinates the operational feasibility and economy of wind power accommodation.

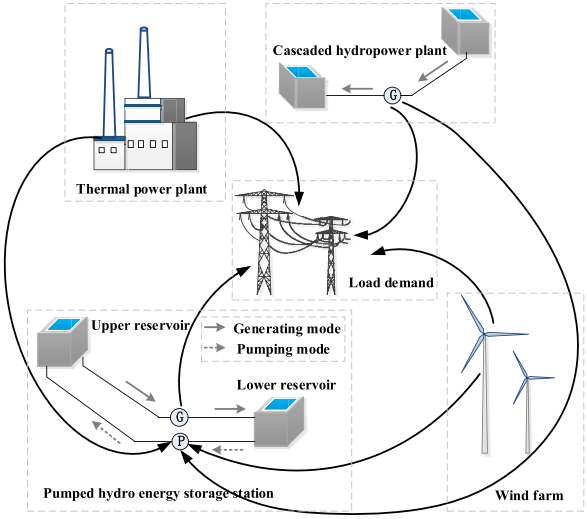

FIGURE 1. A typical WTHS with PHES.

(2) A RSCUC model is proposed based on a developed simplified affine policy so that the realization of uncertainties is strictly coordinated with the decision-making of adjustable variables. Based on linearization techniques, the proposed RSCUC model is transformed into a single-level MILP problem which can be solved directly by efficient commercial solvers and no complex master and subproblem structures are formulated. The computational tractability of the proposed approach in large-scale power systems is verified based on acceleration technique.

(3) Contributions of PHES in economic operation and wind power accommodation are quantitatively evaluated with respect to the WTHS.

The rest of this paper is organized as follows: Section II models the UC problem. Section III provides the linearization method of the proposed model. The proposed approach is verified in section IV. Finally, Section V presents the authors' conclusions.

II. SYSTEM DESCRIPTION AND MATHEMATICAL FORMULATION

A. SYSTEM DESCRIPTION

A typical configuration of a WTHS with PHES is given in Fig. 1. The cascaded hydroelectric system consists of a multi-reservoir at different heights. From the perspective of the electricity market, cascaded HPPs have the advantages of large installed capacity, wide regulation range, and good economic performance. A PHES station is generally composed of upper and lower reservoirs. Unlike a cascaded HPP, a PHES station has reversible pumps. In the coordination operation of a conventional thermal–hydro power system, the PHES station is utilized to smooth the load curves. In the case of a system with significant wind power integration, the PHES station stores surplus energy including that from the wind power during low-load periods by pumping water that is later released during peak-load periods.

B. OBJECTIVE FUNCTION

The goal of the RSCUC model considered in this paper is to absorb prediction error of wind power as much as possible while minimizing the operating cost including the generation cost of thermal and PHES units and the penalty cost of water flow. Hence, the objective function describes the feasibility of wind power accommodation and the economy of the decision results. This is done according to

$$\min\{f_1+f_2+f_3+f_4\} \tag{1}$$

$$f_1=\sum_{t=1}^{T}\sum_{i=1}^{N_G}\left(C_{st,i}u_{i,t}+C_{sd,i}v_{i,t}+f\left(g_{i,t},z_{i,t}\right)+\alpha_i^u\Delta g_{i,t}^u+\alpha_i^l\Delta g_{i,t}^l\right) \tag{2}$$

$$f_2=\sum_{t=1}^{T}\sum_{j=1}^{N_R}\left(\beta_j^u\left(\Delta x_{j,t}^{e,u}-\Delta x_{j,t}^u\right)+\beta_j^l\left(\Delta x_{j,t}^{e,l}-\Delta x_{j,t}^l\right)\right) \tag{3}$$

$$f_3=\sum_{t=1}^{T}\sum_{p=1}^{N_P}\sum_{k=1}^{N_k}\left(C_{pm,k,p}u_{pm,k,p,t}+C_{gn,k,p}u_{gn,k,p,t}\right) \tag{4}$$

$$f_4=\sum_{t=1}^{T}\sum_{h=1}^{N_H}\kappa_h\gamma_h q_{h,t}\Delta t \tag{5}$$

where f_1 is the generation cost of thermal units that includes the fuel cost, start-up and shut-down cost, and reserve cost; f_2 is the penalty cost of curtailment boundaries of wind power; f_3 is the generation cost of PHES units; f_4 is the penalty cost of water flow; $f(g_{i,t}, z_{i,t})$ is the fuel cost of thermal units and is described as a quadratic function typically used in scheduling problem [51].

C. CONSTRAINTS

1) CONSTRAINTS OF THERMAL UNITS

The constraints on the thermal units are given by

$$z_{i,t}-z_{i,t-1}-z_{i,\omega_{st}}\le 0,\quad \forall i,\ \forall t,\ \forall\omega_{st}\in[t,T_{st,i}+t-1] \tag{6}$$

$$z_{i,t-1}-z_{i,t}+z_{i,\omega_{sd}}\le 1,\quad \forall i,\ \forall t,\ \forall\omega_{sd}\in[t,T_{sd,i}+t-1] \tag{7}$$

$$z_{i,t}\in\{0,1\},\quad z_{i,0}=0,\ \forall i,\ \forall t \tag{8}$$

$$z_{i,t}g_i^{\min}\le g_{i,t}\le z_{i,t}g_i^{\max},\quad \forall i,\ \forall t \tag{9}$$

$$g_{i,t}-g_{i,t-1}\le\Delta T\times R_i^{up},\quad g_{i,t-1}-g_{i,t}\le\Delta T\times R_i^{dn},\quad \forall i,\quad \forall t \tag{10}$$

$$0\le\Delta g_{i,t}^u\le\min(z_{i,t}g_i^{\max}-g_{i,t},\Delta T\times R_i^{up}),\quad \forall i,\ \forall t \tag{11}$$

$$0\le\Delta g_{i,t}^l\le\min(g_{i,t}-z_{i,t}g_i^{\min},\Delta T\times R_i^{dn}),\quad \forall i,\ \forall t \tag{12}$$

In the above formulations, constraints (6)–(8) represent the minimum start-up and shut-down time limits. The power generated by a thermal unit is related to its status by the output constraints in (9). Constraints in (10) limit the output between adjacent time periods by the ramp up/down rate. The spinning reserve constraints are given in (11) and (12).

2) CONSTRAINTS OF HYDROPOWER UNITS (HPUS)

The constraints on the HPUs are applied using

$$\sum_{z=1}^{N_{n,h}} e_{z,n,h,t} g^{l}_{z,n,h} \le g_{n,h,t} \le \sum_{z=1}^{N_{n,h}} e_{z,n,h,t} g^{u}_{z,n,h}, \quad \forall z, \quad \forall n \in h, \ \forall h, \ \forall t \tag{13}$$

$$\sum_{z=1}^{N_{n,h}} e_{z,n,h,t} \le 1, \quad \forall z, \ \forall n \in h, \ \forall h, \ \forall t \tag{14}$$

$$g_{n,h,t} = 0.00981 \eta(n_{h,t}, u_{n,h,t}) n_{h,t} u_{n,h,t}, \quad \forall n \in h, \quad \forall h, \ \forall t \tag{15}$$

$$n_{h,t} = h(v_{h,t}) - r(q_{h,t}) - p(u_{n,h,t}), \quad \forall n \in h, \ \forall h, \ \forall t \tag{16}$$

$$v_h^{\min} \le v_{h,t} \le v_h^{\max}, \quad \forall h, \ \forall t \tag{17}$$

$$v_{h,t} = v_{h,t-1} + \left\{ \begin{array}{l} I_{h,t} - q_{h,t} \\ + \sum_{m=1}^{N_m} \left[\begin{array}{l} (1 + \lfloor \tau_m \rfloor - \tau_m) q_{m,t-\lfloor \tau_m \rfloor} \\ + (\tau_m - \lfloor \tau_m \rfloor) q_{m,t-1-\lfloor \tau_m \rfloor} \end{array} \right] \end{array} \right\} \Delta t, \quad \forall m, \quad \forall h, \ \forall t \tag{18}$$

$$q_h^{\min} \le q_{h,t} \le q_h^{\max}, \quad \forall h, \ \forall t \tag{19}$$

$$q_{h,t} = \sum_{n=1}^{N_n} u_{n,h,t} + s_{h,t}, \quad \forall n \in h, \ \forall h, \ \forall t \tag{20}$$

$$0 \le \Delta g^{u}_{n,h,t} \le \sum_{z=1}^{N_{n,h}} e_{z,n,h,t} g^{u}_{z,n,h} - g_{n,h,t}, \quad \forall z, \quad \forall n \in h, \ \forall h, \ \forall t \tag{21}$$

$$0 \le \Delta g^{l}_{n,h,t} \le g_{n,h,t} - \sum_{z=1}^{N_{n,h}} e_{z,n,h,t} g^{l}_{z,n,h}, \quad \forall z, \quad \forall n \in h, \ \forall h, \ \forall t \tag{22}$$

The output constraints of HPUs are described in (13)–(16) where the variable $e_{z,n,h,t}$ determines the operating zone z of unit n of plant h in period t. In (15), $\eta(n_{h,t}, u_{n,h,t})$ is the unit efficiency function, and it is generally obtained from the Hill diagram [52]. For brevity, the power generated by HPP h in period t is denoted as

$$g_{h,t} = \sum_{n=1}^{N_n} g_{n,h,t}, \quad \forall n \in h, \ \forall h, \ \forall t \tag{23}$$

In (16), $h(v_{h,t})$ is a nonlinear function with a fourth-degree polynomial that reflects the forebay level of plant h in period t[53]. Similarly, $r(q_{h,t})$ describes the tailrace level of plant h in period t with a fourth-degree polynomial. The downstream flow is the summation of discharge and spillage where $p(u_{n,h,t})$ is the penstock head loss that can be modeled as a quadratic function of the discharge. Constraints (17)–(20) restrict the reservoir volume and downstream flow. In the water balance constraints in (18), $\lfloor \cdot \rfloor$ is the operator that rounds down to the largest integer that does not exceed the value itself. In this paper, we consider the water delay time as a non-negative real number [17]. The spinning reserve is limited in constraints (21) and (22).

3) CONSTRAINTS OF WIND POWER OUTPUT

The actual output of wind power considering its availability is expressed as constraints according to

$$x^{e}_{j,t} - \varsigma^{l}_{j,t} \Delta x^{l}_{j,t} \le x_{j,t} \le x^{e}_{j,t} + \varsigma^{u}_{j,t} \Delta x^{u}_{j,t}, \quad \forall j, \ \forall t \tag{24}$$

$$\sum_{j=1}^{N_R} \varsigma^{u}_{j,t} \le \Gamma^{u}_{W}, \quad \sum_{j=1}^{N_R} \varsigma^{l}_{j,t} \le \Gamma^{l}_{W} \ \forall j, \ \forall t \tag{25}$$

$$\sum_{t=1}^{T} \varsigma^{u}_{j,t} \le \Gamma^{u}_{T}, \quad \sum_{t=1}^{T} \varsigma^{l}_{j,t} \ge \Gamma^{l}_{T}, \ \forall j, \ \forall t \tag{26}$$

$$\Delta x^{l}_{j,t} \le \Delta x^{e,l}_{j,t}, \quad \Delta x^{u}_{j,t} \le \Delta x^{e,u}_{j,t}, \ \forall j, \ \forall t \tag{27}$$

In practice, it is not common for each wind farm that fluctuates to reach the worst-case in each period. Thus, the binary variables $\varsigma^{u}_{j,t}$ and $\varsigma^{l}_{j,t}$ are introduced to describe the temporal and spatial uncertainties of wind power. In constraints (25) and (26), Γ^{u}_{W} and Γ^{l}_{W} reflect the simultaneity of each wind farm fluctuating at the upper and lower boundaries in each period, respectively. If $\Gamma^{u}_{W} = \Gamma^{l}_{W} = N_R$, $\Gamma^{l}_{T} = 0$, and $\Gamma^{u}_{T} = T$, then the wind power output to be optimized can fluctuate arbitrarily within the predicted boundary. At this time, conservativeness of the wind power output in the spatial dimension can be controlled by adjusting Γ^{u}_{W} and Γ^{l}_{W}. Also, Γ^{u}_{T} and Γ^{l}_{T} determine the conservativeness of wind power output in the temporal dimension. If $\Gamma^{u}_{W} = \Gamma^{l}_{W} = N_R$, $\Gamma^{u}_{T} = 0$, and $\Gamma^{l}_{T} = T$, then the wind power output will fluctuate within the predicted lower boundary (LB), i.e., the actual wind power output does not exceed its predicted value and is conservative. However, if $\Gamma^{u}_{W} > 0$, then Γ^{u}_{T} affects the number of periods in which the wind power output fluctuates within the predicted upper boundary (UB), i.e., the wind power output is optimistic. When $\Gamma^{u}_{W} = \Gamma^{l}_{W} = \Gamma^{l}_{T} = 0$, the model degenerates into the traditional deterministic UC model regardless of the value of Γ^{u}_{T}.

4) CONSTRAINTS OF PHES

The constraints on PHES are established by

$$Q_p^{u,\min} \le Q^{u}_{p,t} \le Q_p^{u,\max}, \quad \forall p, \ \forall t \tag{28}$$

$$Q^{u}_{p,0} = Q^{u}_{p,T}, \quad \forall p, \ \forall t \tag{29}$$

$$Q^{u}_{p,t} = Q^{u}_{p,t-1} + \Delta T \sum_{k=1}^{N_k} (\eta_{pm,k,p} g_{pm,k,p,t-1} - \eta_{gn,k,p} g_{gn,k,p,t-1}), \quad \forall k \in p, \quad \forall k \in p, \ \forall p, \ \forall t \tag{30}$$

$$y_{pm,k,p,t} + y_{gn,k,p,t} \le 1, \quad \forall k \in p, \ \forall p, \ \forall t \tag{31}$$

$$y_{pm,k,p,t} g^{\min}_{pm,k,p} \le g_{pm,k,p,t} \le y_{pm,k,p,t} g^{\max}_{pm,k,p}, \quad \forall k \in p, \quad \forall p, \ \forall t \tag{32}$$

$$y_{gn,k,p,t} g^{\min}_{gn,k,p} \le g_{gn,k,p,t} \le y_{gn,k,p,t} g^{\max}_{gn,k,p}, \quad \forall k \in p, \quad \forall p, \ \forall t \tag{33}$$

$$y_{pm,k,p,t} + y_{gn,k,p,t+1} \le 1, \quad \forall k \in p, \ \forall p, \ \forall t, \ \forall t \in [1, T-1] \tag{34}$$

$$y_{pm,k,p,t+1} + y_{gn,k,p,t} \le 1, \quad \forall k \in p, \ \forall p, \ \forall t, \ \forall t \in [1, T-1] \tag{35}$$

$$y_{pm,k,p,t} + y_{gn,k,p,t+2} \le 1, \quad \forall k \in p,\ \forall p,\ \forall t, \ \forall t \in [1, T-2] \tag{36}$$

$$y_{pm,k,p,t+2} + y_{gn,k,p,t+1} \le 1, \quad \forall k \in p, \quad \forall p,\ \forall t,\ \forall t \in [1, T-2] \tag{37}$$

$$0 \le \Delta g^{u}_{pm,k,p,t} \le g_{pm,k,p,t} - y_{pm,k,p,t} g^{\min}_{pm,k,p}, \quad \forall k \in p, \quad \forall p,\ \forall t \tag{38}$$

$$0 \le \Delta g^{l}_{pm,k,p,t} \le y_{pm,k,p,t} g^{\max}_{pm,k,p} - g_{pm,k,p,t}, \quad \forall k \in p, \quad \forall p,\ \forall t \tag{39}$$

$$0 \le \Delta g^{u}_{gn,k,p,t} \le y_{gn,k,p,t} g^{\max}_{gn,k,p} - g_{gn,k,p,t}, \quad \forall k \in p, \quad \forall p,\ \forall t \tag{40}$$

$$0 \le \Delta g^{l}_{gn,k,p,t} \le g_{gn,k,p,t} - y_{gn,k,p,t} g^{\min}_{gn,k,p}, \quad \forall k \in p, \quad \forall p,\ \forall t \tag{41}$$

Reservoir volumes of PHES stations are restricted by constraints (28) and (30). In assumption, the volumes of the upper reservoir are restricted as long as the total volume of the reservoirs is constant. Equation (30) formulates the upper reservoir volumes. The constraints in (31) describe the operating mode of a PHES unit. In (31), if $y_{pm,k,p,t} = 1$, the PHES unit works in the pumping mode. If $y_{gn,k,p,t} = 1$, PHES unit works in the generating mode. Otherwise, the PHES unit is idle. Power generated by a PHES unit both in pumping and in generating modes is limited by the constraints of (32) and (33). PHES units generally do not switch continuously between pumping and generating modes, and they need to remain idle for at least half an hour. Considering this, the constraints on operating modes conversion time is given in (34)–(37). The spinning reserve is limited in constraints (38)–(41).

5) CONSTRAINTS OF POWER SYSTEM

The power system constraints are defined according to

$$\sum_{i=1}^{N_G} g_{i,t} + \sum_{h=1}^{N_H} g_{h,t} + \sum_{j=1}^{N_R} x^{e}_{j,t} + \sum_{p=1}^{N_P}\sum_{k=1}^{N_K} (g_{gn,k,p,t} - g_{pm,k,p,t}) = D_t, \quad \forall i, \quad \forall h,\ \forall j,\ \forall k \in p,\ \forall p,\ \forall t \tag{42}$$

$$\sum_{r=1}^{N_S} \Delta g^{u}_{r,t} \ge \sum_{j=1}^{N_R} \varsigma^{l}_{j,t} \Delta x^{l}_{j,t}, \quad \forall r,\ \forall j,\ \forall t \tag{43}$$

$$\sum_{r=1}^{N_S} \Delta g^{l}_{r,t} \ge \sum_{j=1}^{N_R} \varsigma^{u}_{j,t} \Delta x^{u}_{j,t}, \quad \forall r,\ \forall j,\ \forall t \tag{44}$$

$$-L^{\max}_{s} \le \sum_{r=1}^{N_S} \lambda_{r,s}(g_{r,t} + \Delta g_{r,t}) + \sum_{j=1}^{N_R} \lambda_{j,s}(x^{e}_{j,t} + \Delta x_{j,t}) \le L^{\max}_{s}, \quad \forall s, \quad \forall r,\ \forall j,\ \forall t \tag{45}$$

Equation (42) provides the power balance constraints. The spinning reserve constraints are expressed in (43) and (44). For brevity, N_S represents the total number of conventional units plus the PHES units. Constraints in (45) ensure the security of the transmission lines.

III. LINEARIZATION OF THE PROPOSED MODEL

A. FUEL COST LINEARIZATION OF THERMAL UNITS

The fuel cost of a thermal unit is generally described as

$$f\left(g_{i,t}, z_{i,t}\right) = a_i g^{2}_{i,t} + b_i g_{i,t} + c_i z_{i,t} \tag{46}$$

The quadratic function in (46) can be approximated by a set of piecewise linear functions obtained by the method presented in [55] and [56], as shown below.

$$\begin{cases} f\left(g_{i,t}, z_{i,t}\right) = f\left(g^{\min}_{i}, z_{i,t}\right) + \sum_{o=1}^{N_o} \xi_{o,t}\omega_{o,t} \\ 0 \le \omega_{o,t} \le g^{o}_{i,t} - g^{o-1}_{i,t}, \quad \forall i,\ \forall t,\ \forall o \end{cases} \tag{47}$$

where N_o is segment numbers of power generated by a thermal unit, $\xi_{o,t}$ and $\omega_{o,t}$ are the slope and output of segment o in period t.

B. STATE CONVERSION OF THERMAL UNITS

The relaxation variables u_{it} and v_{it} are introduced to linearize the logical relationship between the start-up and shut-down status of thermal units, and the conversion can be expressed as

$$\begin{cases} z_{i,t} - z_{i,t-1} - u_{i,t} \le 0 \\ z_{i,t-1} - z_{i,t} - v_{i,t} \le 0 \\ u_{i,t}, v_{i,t}, z_{i,t} \in \{0, 1\}, \quad \forall i,\ \forall t \end{cases} \tag{48}$$

In the constraints in (48), if $u_{it} = 1$, unit i will have started up in period t; and if $v_{it} = 1$, unit i will be shut down in period t. The method for linearizing the operating status of a PHES unit is similar to the thermal unit and will not be described in detail in this section.

C. LINEARIZATION OF HPU CONSTRAINTS

In this paper, the heuristic algorithm presented by Guedes *et al.* [18] is employed to preprocess the UC problem of HPUs. The heuristic algorithm is based on the rules for the use of downstream flow that determine the power generated by each HPU in each period according to the maximum efficiency or the maximum discharge. Compared with the formulation presented by [57], linear complexity is the main advantage of the heuristic algorithm since the power generated by the HPU is approximated by rectangles instead of triangles. On this basis, a robust UC model of HPUs is formulated with a series of linear constraints defined by convex combination parameters according to

$$g_{h,t} - \sum_{\upsilon=1}^{R_h+1}\sum_{\sigma=1}^{U_h+1} G_{h,\sigma,\upsilon}\chi_{\sigma,\upsilon,h,t} = 0, \quad \forall h,\ \forall t,\ \forall \upsilon,\ \forall \sigma \tag{49}$$

$$q_h^{\min} \le \sum_{\upsilon=1}^{R_h+1}\sum_{\sigma=1}^{U_h+1} Q_{h,\sigma}\chi_{\sigma,\upsilon,h,t} \le q_h^{\max}, \quad \forall h,\ \forall t,\ \forall \upsilon,\ \forall \sigma \tag{50}$$

$$v_h^{\min} \le 2\sum_{\sigma=1}^{U_h+1}\sum_{\upsilon=1}^{R_h+1} V_{h,\upsilon}\chi_{\sigma,\upsilon,h,t} - v_{h,t-1} \le v_h^{\max}, \quad \forall h,\ \forall t,\ \forall \upsilon,\ \forall \sigma \tag{51}$$

$$\begin{cases} \sum_{\sigma=1}^{U_h+1}\sum_{\xi=1(\xi\neq\upsilon,\upsilon+1)}^{R_h+1} \chi_{\sigma,\xi,h,t} + d^x_{\upsilon,h,t} \le 1 \\ \sum_{\upsilon=1}^{R_h+1}\sum_{\xi=1(\xi\neq\sigma,\sigma+1)}^{U_h+1} \chi_{\xi,\upsilon,h,t} + d^y_{\sigma,h,t} \le 1 \\ \sum_{\upsilon=1}^{R_h} d^x_{\upsilon,h,t} = 1 \\ \sum_{\sigma=1}^{U_h} d^y_{\sigma,h,t} = 1 \\ \sum_{\upsilon=1}^{R_h+1}\sum_{\sigma=1}^{U_h+1} \chi_{\sigma,\upsilon,h,t} = 1 \\ d^x_{\upsilon,h,t}, d^y_{\sigma,h,t} \in \{0,1\},\ \chi_{\sigma,\upsilon,h,t} \ge 0, \quad \forall h,\ \forall t,\ \forall \upsilon,\ \forall \sigma \end{cases} \tag{52}$$

The modified constraints of hydropower output, downstream flow, and reservoir volume are described in (49)–(51). The auxiliary variables are defined and limited by the constraints in (52). Among them, if $d^x_{\upsilon,h,t} = 1$ and $d^y_{\sigma,h,t} = 1$, then the reservoir volume $v_{h,t}$ is kept within $[V_{h,\upsilon}, V_{h,\upsilon+1}]$, the downstream flow $q_{h,t}$ is kept within $[Q_{h,\sigma}, Q_{h,\sigma+1}]$, and the hydropower $g_{h,t}$ is dependent on the convex combination of $G_{h,\sigma,\upsilon}$ and $\chi_{\sigma,\upsilon,h,t}$

D. LINEARIZATION OF SPINNING RESERVE CONSTRAINTS

The right-hand side of constraints (43) and (44) include bilinear terms that multiply two decision variables. In this paper, we address these bilinear terms by introducing the auxiliary variables $\theta^u_{r,t}$ and $\theta^l_{r,t}$ by

$$\begin{cases} \sum_{r=1}^{N_S} \theta^u_{r,t} = \sum_{j=1}^{N_R} \varsigma^u_{j,t}\Delta x^u_{j,t} \\ \sum_{r=1}^{N_S} \theta^u_{r,t} = \sum_{j=1}^{N_R} \varsigma^l_{j,t}\Delta x^l_{j,t}, \quad \forall j,\ \forall t,\ \forall r \end{cases} \tag{53}$$

The physical meaning of $\theta^u_{r,t}$ and $\theta^l_{r,t}$ can be interpreted as the minimum downward and upward regulating power provided by the adjustable unit r in period t. Equation (53) is derived from a simplified affine policy [32] where the regulating power of the adjustable unit is formulated as

$$\Delta g_{r,t} = \varpi_{r,t}\sum_{j=1}^{N_R}\Delta x_{j,t} \quad \forall j,\ \forall t,\ \forall r \tag{54}$$

where $\varpi_{r,t}$ is a coefficient reflecting the participation sensitivity of adjustable unit r in period t. As (53) avoids the newly introduced decision variable, the constraints in (43) and (44) can be expanded to linear constraints according to

$$\begin{cases} \Delta g^u_{r,t} \ge \theta^l_{r,t} \\ \Delta g^l_{r,t} \ge \theta^u_{r,t} \\ \sum_{r=1}^{N_S}\theta^l_{r,t} \le \sum_{j=1}^{N_R}\varsigma^l_{j,t}\Delta x^{e,l}_{j,t} \\ \sum_{r=1}^{N_S}\theta^u_{r,t} \le \sum_{j=1}^{N_R}\varsigma^u_{j,t}\Delta x^{e,u}_{j,t}, \quad \forall j,\ \forall t,\ \forall r \end{cases} \tag{55}$$

E. LINEARIZATION OF SECURITY CONSTRAINTS

The constraints in (45) contain the uncertain variables $\Delta g_{r,t}$ and $\Delta x_{j,t}$. In this paper, Soyster's method [58] is employed to eliminate the uncertainty variables. Also, according to the duality theory [59], auxiliary variables $J_{j,t}$, $l_{j,t}$, and $\varphi_{j,t}$ are introduced to transform (45) into deterministic constraints.

$$\begin{cases} \sum_{j=1}^{N_R}\left(\lambda_{j,s}\Delta x^u_{j,t} + J_{j,t}\right) + \sum_{r=1}^{N_S}\lambda_{r,s}\Delta\theta^u_{r,t} \ge L_s^{\max,l} \\ J_{j,t} \le \min\left(0, -\left(\lambda_{j,s}\left(\Delta x^u_{j,t} + \Delta x^l_{j,t}\right) + \sum_{r=1}^{N_S}\lambda_{r,s}\varphi_{j,t}\right)\right) \\ \sum_{j=1}^{N_R}\left(\lambda_{j,s}\left(-\Delta x^l_{j,t}\right) + l_{j,t}\right) + \sum_{r=1}^{N_S}\lambda_{r,s}\left(-\Delta\theta^l_{r,t}\right) \le L_s^{\max,u} \\ l_{j,t} \ge \max\left(0, \lambda_{j,s}\left(\Delta x^u_{j,t} + \Delta x^l_{j,t}\right) + \sum_{r=1}^{N_S}\lambda_{r,s}\varphi_{j,t}\right) \\ \sum_{j=1}^{N_R}\varphi_{j,t} = \Delta\theta^u_{r,t} + \Delta\theta^l_{r,t} \\ L_s^{\max,l} = -L_s^{\max} - \sum_{r=1}^{N_S}\lambda_{r,s}g_{r,t} - \sum_{j=1}^{N_R}\lambda_{j,s}x^e_{j,t} \\ L_s^{\max,u} = L_s^{\max} - \sum_{r=1}^{N_S}\lambda_{r,s}g_{r,t} - \sum_{j=1}^{N_R}\lambda_{j,s}x^e_{j,t}, \quad \forall j,\ \forall t,\ \forall r,\ \forall s \end{cases} \tag{56}$$

Finally, the proposed model is converted into a MILP model that can be solved by an existing commercial software package.

As can be seen in (56), the introduced auxiliary variables are closely related with scale, i.e. the number of units and transmission lines, which increase the computational requirements. However, only a few constraints in (56) are active in practice [34], so we can eliminate the redundant constraints to improve computational efficiency for large-scale problems. Here, an acceleration technique presented in [34] is adopted in this paper with minor modification.

Considering the following problems to find the violated constraints:

$$\max\left\{\sum_{r=1}^{N_S}\lambda_{r,s}\Delta g_{r,t} + \sum_{j=1}^{N_R}\lambda_{j,s}\Delta x_{j,t}\right\} > L_s^{\max,u} \tag{57}$$

$$\min\left\{\sum_{r=1}^{N_S}\lambda_{r,s}\Delta g_{r,t}+\sum_{j=1}^{N_R}\lambda_{j,s}\Delta x_{j,t}\right\}<L_s^{\max,l} \quad (58)$$

$$s.t.\ -\Delta g_{r,t}^{l}\le\Delta g_{r,t}\le\Delta g_{r,t}^{u},\quad \forall t,\ \forall r \quad (59)$$

$$-\varsigma_{j,t}^{l}\Delta x_{j,t}^{l}\le\Delta x_{j,t}\le\varsigma_{j,t}^{u}\Delta x_{j,t}^{u},\quad \forall j,\ \forall t, \quad (60)$$

$$\psi(s)=\left\{L_s^{\max,u},L_s^{\max,l},\Delta g_{r,t}^{u},\Delta g_{r,t}^{l},\varsigma_{j,t}^{u},\varsigma_{j,t}^{l},\Delta x_{j,t}^{u},\Delta x_{j,t}^{l}\right\} \quad (61)$$

where (57)–(61) are linear programming (LP) problems which can be solved efficiently by using a commercial solver. $\psi(s)$ is a feasible set obtained by the MILP model with a subset of constraints (56). The detail of the procedure can be referred to [34].

IV. CASE STUDY

A. CASE DESCRIPTION

Numerical results of the proposed approach are presented on three modified standard test systems. To investigate the impact of some related factors on the economic operation and wind power accommodation, numerical tests are run on a modified IEEE-30 bus system [60]. The thermal units are connected through buses 1, 2, 13, 22, and 23. The wind farm is connected through bus 5, the PHES unit through bus 11, and the HPP through bus 27. Thermal units are numbered from G1 to G5. Fig. 2 in the Appendix gives the predicted output of load and wind power. The wind power data is derived from EirGrid [61], and the data from February 3, 2016, is used as the predicted value for an equivalent installed capacity of 420 MW. The boundary of the wind power prediction error is selected as the 95% confidence interval of the empirical distribution proposed by Ma *et al*. [62].

The load demand curve is obtained by converting a typical daily load curve of a provincial power grid in southwest China to the capacity of the simulation system. The penalty costs of wind power curtailment and load shedding are 80 \$/MWh and 120 \$/MWh, the start-up cost in both the power generating and pumping modes is \$300, and the penalty cost of water flow is 6.94×10^{-3} \$/($m^3\cdot s$).

The unit parameters of the HPPs with reservoirs are given by Guedes *et al*. [18]. The total installed capacity of HPPs is 930 MW. In this paper, units in the Nova Ponte plant are numbered from P1 to P3, and in the Miranda plant, they are numbered from M1 to M3. Inflows of these two plants are derived from Instance 48-1 by linear interpolation. The parameters of the thermal and PHES units are listed in Table 1 and Table 2 in the Appendix.

To demonstrate the computational efficiency of the proposed approach, numerical tests are implemented on the modified IEEE 118-bus [63] and the Polish 2736-bus systems [64]. The modified IEEE 118-bus system has 52 thermal units, 6 HPUs, 2 PHES units, and 186 transmission lines. Four wind farms are connected to the system at bus 17 (400 MW), 37 (400 MW), 66 (500 MW), and 81 (400 MW). The modified Polish 2736-bus system has 134 thermal units (25801.7 MW of total capacity), 12 HPUs (1860 MW of total capacity), 4 PHES units (2400 MW of total capacity), 72 wind farms which are located at different buses (12960 MW of total capacity), and 3504 transmission lines. All the hourly data of wind power are obtained from EirGrid and the hourly load demands are obtained from [63]. The proposed model is solved by Gurobi 8.1 [65] on a notebook with an Intel Core i7 at 2.70 GHz and 8 GB RAM. The MIP gap is set to be 0.01%.

TABLE 1. Adjustable capacities of various power supplies at different temporal uncertainty budgets.

Γ_T^u	Case 1	Case 2
	Thermal/Hydro/PHES (MWh)	Thermal/Hydro/PHES (MWh)
0	21.14; 0; 988.70	0;55.65;954.19
24	124.56; 0; 1,211.62	0; 324.44; 1017.24
48	232.41; 0; 1407.09	0; 545.29; 1098.38
72	340.22; 0; 1572.14	0; 723.62 ; 1196.06
96	506.68; 0; 1656.00	0; 1059.21; 1103.46

TABLE 2. TPT and TPH in various cases at different ramp rate levels.

Ramp rete level	Case 1	Case 2	Case 3	Case 4
	TPT/TPH	TPT/TPH	TPT/TPH	TPT/TPH
0.95	480; 506	480; 502	480; 462	480; 487
1.00	390; 506	352; 506	478; 460	359; 494

B. IMPACT OF UNCERTAINTY BUDGET

The ideal situation where wind power prediction is accurate enough allows the traditional deterministic UC model to be realized. At this time, the system operators give the scheduling plan according to the economic performance of conventional units. To measure the economic performance in different operating scenarios, this paper defines the economic index as

$$I_e=\frac{C_{test}-C_{ideal}}{C_{ideal}} \quad (62)$$

where C_{test} is the operating cost of the test case and C_{ideal} is the operating cost for the ideal situation. When the test case has a feasible solution, wind power prediction error causes I_e to always be greater than 0. The economy of the test case worsens in proportion to the I_e value.

This paper defines the wind power accommodation index I_a to evaluate the utilization of wind power according to

$$I_a=\frac{\sum_{t=1}^{T}\sum_{j=1}^{N_R}\left(\Delta x_{j,t}^{u}-\Delta x_{j,t}^{l}\right)}{\sum_{t=1}^{T}\sum_{j=1}^{N_R}\left(\varsigma_{j,t}^{u}\Delta x_{j,t}^{e,u}-\varsigma_{j,t}^{l}\Delta x_{j,t}^{e,l}\right)} \quad (63)$$

In practice, cascaded HPP as an excellent peak-shaving power supply that usually operates as an automatic generation

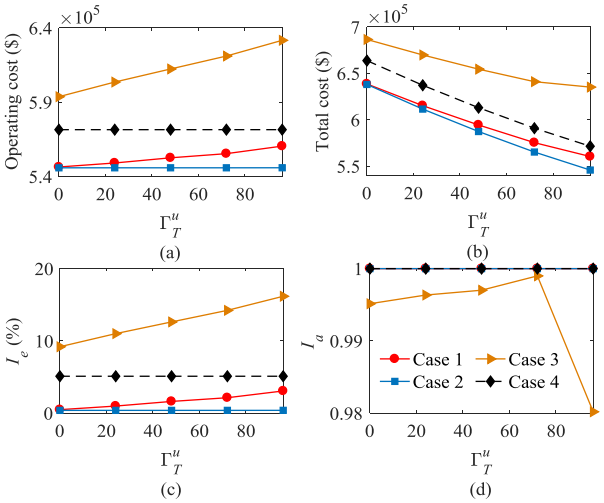

FIGURE 2. Results for different temporal uncertainty budgets.

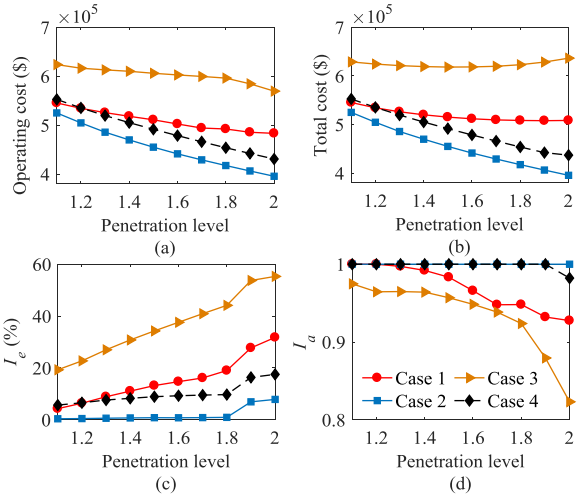

FIGURE 3. Results for different wind power penetration levels.

control (AGC) unit in the dry season. However, during the flood season, the HPU must reach its maximum power output as fast as possible due to economic and the security reasons [66], resulting in the HPU having no AGC capability. Therefore, the numerical tests in this paper consider that a HPP has these two operating modes and defines the following operating scenarios:

Case 1: with PHES and HPUs have no AGC capabilities.
Case 2: with PHES and HPUs have AGC capabilities.
Case 3: no PHES and HPUs have no AGC capabilities.
Case 4: no PHES and HPUs have AGC capabilities.

The optimism of the wind power prediction is determined by Γ_T^u. Fig. 2 shows the variations in cost and index of different operating modes for different temporal uncertainty budgets Γ_T^u (where $\Gamma_T^l = 48$, $\Gamma_W^u = \Gamma_W^l = 1$).

In the cases where HPUs have no AGC capabilities, the operating costs increase with the increase of temporal uncertainty budgets, and the operating point of the thermal unit is offset from the economic optimal to the robust optimal (Fig. 2(a)). However, if the HPUs have AGC capabilities, the operating costs are hardly affected by the temporal uncertainty budgets. For the same uncertainty budget, cases without PHES are significantly impacted depending on whether the HPUs have AGC capabilities or not. However, with PHES, the presence of HPUs with AGC capabilities has a slightly weaker impact on the operating costs and the total costs as seen in Fig. 2(a) and 2(b). Thus, the robustness of the scheduling plan is enhanced with PHES. This can also be seen from the economic indices in Fig. 2(c) that shows the operating modes without PHES are higher at the same uncertainty budget. Fig. 2(d) indicates that, except for Case 3, the accommodation indices of wind power are almost the same. Specifically, for HPUs with AGC capabilities, the PHES improves the economics of the power system's operation by an average of 4.72%. Whereas in Case 3, the wind power uncertainties are not fully compensated by the thermal units. When the HPUs have no AGC capabilities, the contributions of PHES are reflected in an average increase in the economic performance of the system by 10.98% and an extension of the admissible interval of wind power by 0.65%.

Table 1 lists the adjustable capacities provided by conventional and PHES units at different temporal uncertainty budgets. The adjustable capacities of these power generation supplies rise with the increase of temporal uncertainty budgets. HPUs with AGC capabilities reduce the adjustable capacities supplied by PHES. For a temporal uncertainty budget of $\Gamma_T^u = 48$, the adjustable capacities supplied by a PHES decrease by 21.94%.

C. IMPACT OF WIND POWER PENETRATION

In this section, we discuss and evaluate the accommodation ability of wind power as its penetration increases. To evaluate the maximum capacity of wind power to be absorbed, Γ_T^u is taken as 96. The wind power penetration level is the ratio of wind power output to the initial forecasted value and is varied between 1.1 and 2.0. The computed results are given in Fig. 3.

The operating costs and total costs are reduced as penetration levels of wind power increase as seen in Fig. 3(a) and 3(b). The economic indices gradually increase with the increase of wind power penetration level as shown in Fig. 3(c). The increase is caused by the system having to sacrifice economy to cope with the increasing wind power fluctuations. Fig. 3(d) indicates that the ability to respond to wind power fluctuations by conventional units is limited, especially for high wind power penetration. For HPUs with no AGC capabilities, PHES improves the economic performance from 15.00% to 26.00% and increases the wind power accommodation from 2.52% to 10.43% as the wind power penetration level increases. When the HPUs have AGC capabilities, PHES increases the economic performance from 5.28% to 9.66%.

Fig. 4 shows the accommodation results for the wind power penetration level of 2. In this figure, the dashed light blue line represents the predicted UB of wind power, and the solid

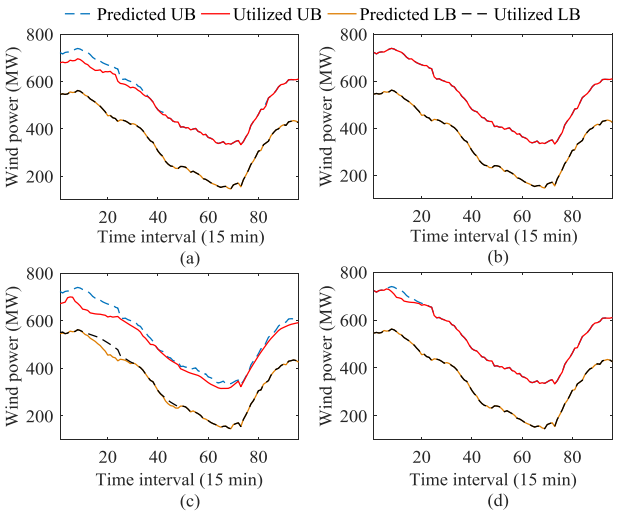

FIGURE 4. Accommodation results of wind power predicted intervals. (a) Case 1. (b) Case 2. (c) Case 3. (d) Case 4.

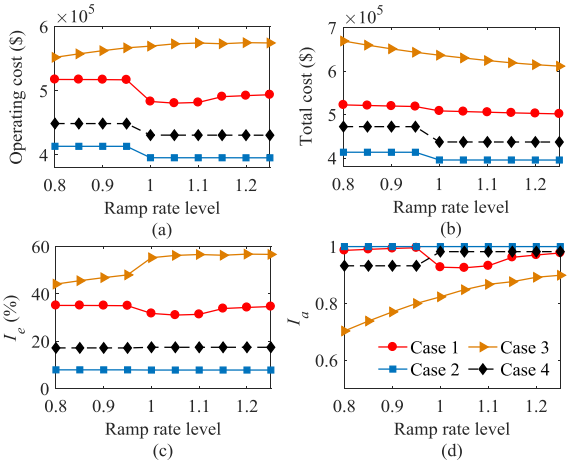

FIGURE 5. Results for different ramp rate levels.

orange line represents the predicted LB of wind power. The admissible interval of wind power consists of the utilized UB (solid red line) and LB (dashed black line). Notice that the accommodation of the wind power predicted interval could not be fully realized, except for Case 2 as seen in Fig. 4(b). For Fig. 4(a), 4(b), and 4(c), the time periods in which the wind power predicted intervals could not be completely absorbed are concentrated in the low-load periods due to the insufficient peak-shaving capacity.

D. RELATED ANALYSIS WITH HIGH WIND POWER PENETRATION

1) RAMP UP/DOWN RATE

The ramp rate is an important parameter of a thermal unit that reflects the adjustable speed of the thermal unit in response to wind power fluctuations. Fig. 5 shows the results for a wind power penetration level of 2. The ramp rate level is the ratio of ramp rate over its original value listed in Table 1 in the Appendix.

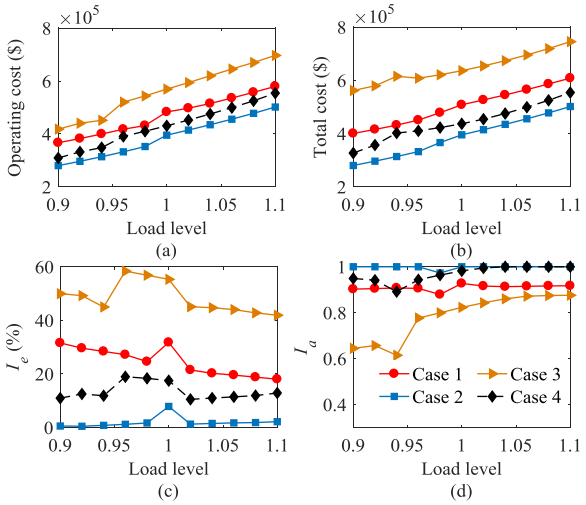

FIGURE 6. Results for different load levels.

Fig. 5 shows that there is a considerable increase both in operating cost and in wind power utilization in Case 3 when the ramp rate level changes from 0.8 to 1.25. Compared to Case 3, wind power fluctuations can be compensated in Case 1 with operating cost savings from 9.00% to 25.27% showing the benefit of PHES. In Case 4, the wind power accommodation indices change with the increase in ramp rate levels of thermal units. Whereas in Case 2, the ramp rate level mainly affects the operating costs or total costs. The system economic indices Ie for Case 2 do not change greatly, and the wind power accommodation indices I_a remain stable. Compared to Case 4, the economic performance of Case 2 is improved from 9.24% to 9.61% as the wind power accommodation is increased from 1.78% to 6.76%.

For the increase of the ramp rate level from 0.95 to 1.00, there is a decrease in wind power accommodation for Case 1 and an increase for Case 4. This can be explained by Table 2. The total online periods of thermal units (TPT) in Case 1 are reduced due to the increase of the ramp rate. Whereas in Case 4, the total online periods of hydropower units (TPH) are increased due to the AGC capability provided by HPUs that improves the wind power utilization.

2) LOAD DEMAND

This section explores the impact of load demand on wind power accommodation. The load level is defined as a ratio of load demand over the forecasted value and is varied from 0.9 to 1.1 in this study. Fig. 6 shows the computed results of varying load level for a wind power penetration level of 2. As can be seen in this figure, the operating costs obtained in Case 2 are considerably lower than those of Case 3. This difference is a result of the regulation capacity supported by PHES and cascaded HPPs Even so, the operating costs in these operating scenarios rise with the increase of load level. This increase is consistent with real-world observations. The load level also has a significant impact on wind power accommodation.

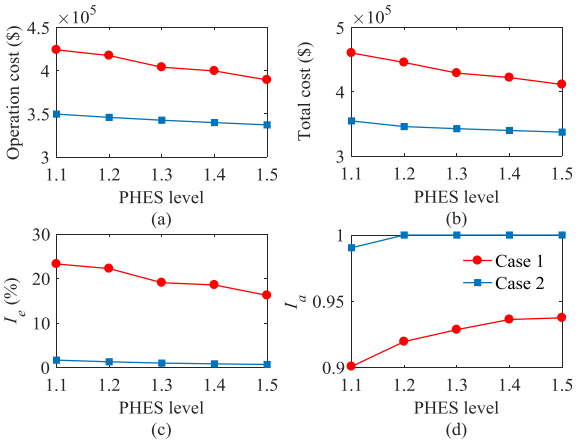

FIGURE 7. Results for different PHES levels.

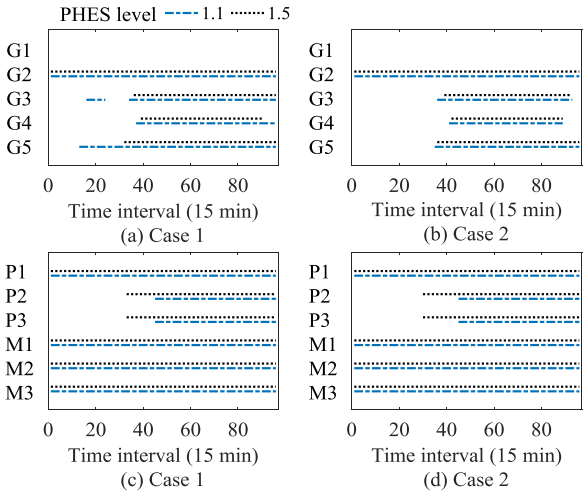

FIGURE 8. UC results of conventional units at different PHES levels. (a) Case 1. (b) Case 2. (c) Case 1. (d) Case 2.

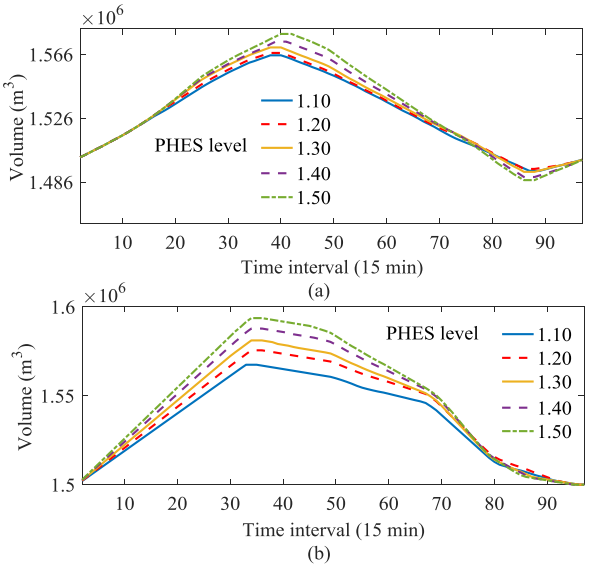

FIGURE 9. Reservoir volume curve of the PHES station. (a) Case 1. (b) Case 2.

For HPUs with no AGC capabilities, the PHES increases the economic performance from 16.58% to 32.25% and the wind power accommodation from 4.13% to 25.78%. Whereas in the cases that HPUs provide AGC capacities, the PHES improves the economic performance from 9.24% to 17.74%, and the wind power accommodation from 0.53% to 10.83%. Thus, the PHES greatly improves wind power utilization and the economic performance.

3) CAPACITY LIMIT OF PHES

The analysis in the previous section shows that the wind power predicted intervals could not be fully absorbed for each operating scenario for a wind power penetration level of 2.0 and load level of 0.98 with the used current capacity configuration of PHES. Here, the PHES level which is defined as the ratio between the capacity limit of PHES and its initial installed capacity is varied from 1.1 to 1.5. Fig. 7 shows the trends in the costs and indices when varying the PHES level in this range. This figure shows that increasing capacity limit of PHES improves the economics of the power system operation and the accommodation of wind power. These improvements are seen regardless of whether HPU is an adjustable power generation resource or not.

In cases with HPUs that have no AGC capabilities, an increase of PHES level improves economic performance from 34.47% to 44.52%, and wind power accommodation from 10.14% to 13.81%. When HPUs have AGC capabilities, the economic performance improved from 17.46% to 21.06% and the wind power accommodation improved from 2.65% to 3.61% with the increase of PHES level from 1.1 to 1.5.

Fig. 8 shows the UC results of conventional units when the PHES levels are 1.1 and 1.5. A change in PHES level affects the online time periods of conventional units.

Variations in the reservoir volume of PHES are shown in Fig. 9. An increase of the PHES capacity limit increases the water exchanged by the upper reservoir for both the pumping and generating modes. As a result, the system's peak-shaving capability is enhanced. This further explains the improvements in the economics and wind power accommodation with different PHES levels observed in Fig. 7.

E. COMPUTATIONAL EFFICIENCY

This section presents the computational efficiency of the proposed approach on the medium and large-scale power systems, i.e. the modified IEEE 118-bus and the Polish 2736-bus systems.

1) SEGMENT NUMBERS IN LINEARIZATION

The impact of segment numbers on total cost and solver time is discussed in the 118-bus system. Without loss of generality, $\Gamma_T^u = \Gamma_T^l = T/2$ and $\Gamma_W^u = \Gamma_W^l = N_R/2$. The segment numbers of thermal units and HPUs are varied from 2 to 16. The computed results are shown in Fig. 10 when varying the segment number in this range. As can be seen in this figure,

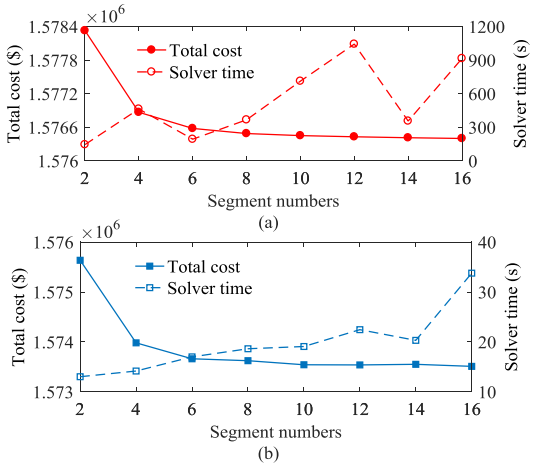

FIGURE 10. Results for different segment numbers in 118-bus system. (a) Case 1. (b) Case 2.

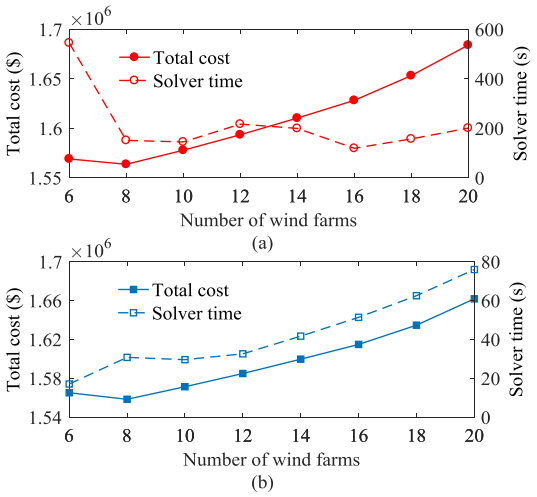

FIGURE 11. Results for different numbers of wind farms in 118-bus system. (a) Case 1. (b) Case 2.

the total cost decreases as the segment number increases. The total costs obtained in Case 2 are considerably lower than those of Case 1 due to the regulation capacity supported by cascaded HPUs. For the same segment number in each case, less solver time is spent in Case 1. When the segment number varies from 8 to 16, the reduction in total cost gradually tends to stabilize. However, the increasing segment number increases the solver time. These observations indicate that the segment number of 8 is applicable for the test system to obtain an accurate result with high solution efficiency.

2) NUMBER OF WIND FARMS

This section explores the impact of the number of wind farms on computational efficiency in the 118-bus system. For illustration, we add 16 wind farms with a capacity of 100 MW to the test system. Figure 11 shows the trends in total costs and solver time when the total number of the integrated wind farms increases from 6 to 20. It can be seen from the figure that when the total number of integrated wind farms

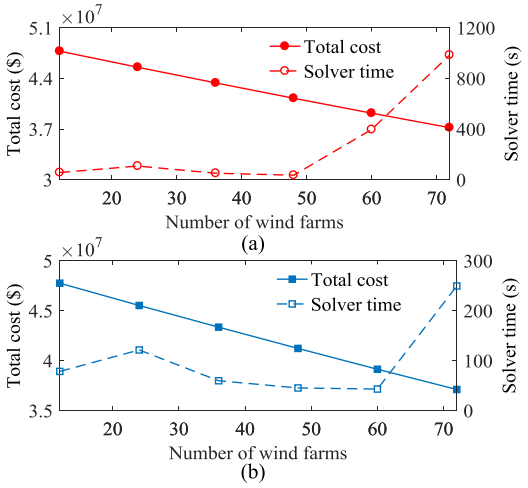

FIGURE 12. Results for different numbers of wind farms in 2736-bus system. (a) Case 1. (b) Case 2.

reaches 8, the total cost in each operating scenario has an inflection point where the increment of penalty cost of curtailment boundaries of wind power begins to be greater than the reduction of operating cost. Meanwhile, the solver time spent in Case 2 is considerably less than that of Case 1, although there are more decision variables in Case 2. On average, the solver time of case 1 is around 217.08 s and that of case 2 is around 42.72 s. Moreover, solver time has an increasing trend in case 2; even so, it is less than 80 s.

3) SCALE OF TEST SYSTEM

The impact of the scale of power system on computational efficiency is tested on the 2736-bus system. Also, we discuss the impact of the number of wind farms on computational results. Fig. 12 shows the trends in total cost and solver time when increasing the number of wind farms from 12 to 72. Variations in the number of wind farms affect the total cost and the solver time in both operating scenarios. It is observed that when the number of wind farms is not more than 48, the solver time of the proposed approach is irrelevant to the system scale in both operating scenarios. However, the solver time increases gradually as the number of wind farms varies from 60 to 72, where the average solver time of case 1 is around 690.74 s and that of case 2 is around 146.37 s. Compared with the 118-bus system, the solver time of the 2736-bus system does not increase by an order of magnitude, which is mainly due to the adoption of acceleration technique to eliminate about 86.95%∼ 95.19% constraints of the transmission lines in the large-scale power system. From the observed test results, the computational efficiency indicates that the proposed approach is promising for the short-term scheduling in large-scale WTHS including PHES.

V. CONCLUSION

In this paper, we propose a MILP based RSCUC model to solve the short-term scheduling problem of WTHS

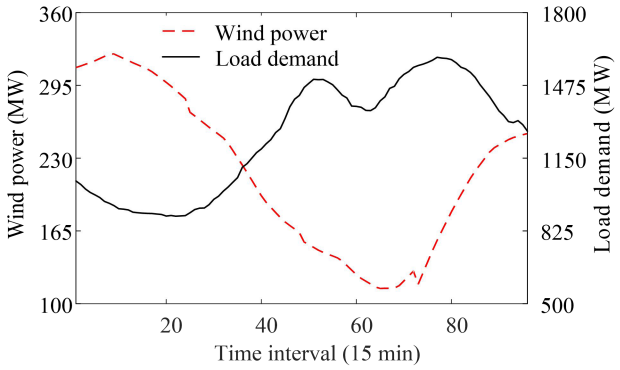

FIGURE 13. Predicted wind power and load demand.

TABLE 3. Parameters of thermal units.

Parameters	G1	G2	G3	G4	G5
g^{max}/MW	300	200	100	80	50
g^{min}/MW	60	40	20	16	10
a/(\$/MW^{2}h)	0.052	0.05	0.018	0.0148	0.01
b/(\$/MWh)	38.4	25.76	32.8	34.4	28.8
c/(\$/h)	220	160	200	150	170
C_{st}/\$	400	333.33	200	200	100
C_{sd}/\$	200	166.67	100	100	50
T_{st}/h	5	2	1.5	1	1
T_{sd}/h	5	2	1.5	1	1
R^{up}/(MW/h)	88	80	80	64	40
R^{dn}/(MW/h)	88	80	80	64	40

including PHES. In this approach, the admissible interval of wind power is optimized. The conservativeness of the RSCUC model is adjustable by introducing uncertainty budgets over temporal and spatial dimensions. Moreover, acceleration technique is adopted to improve computational efficiency for large-scale problems. Numerical tests demonstrate the effectiveness and computational tractability of the proposed approach. Related factors, such as uncertainty budgets and wind power penetration levels affect the economic operation of the system and the utilization of wind power. Under high wind power penetration, the ramp rate of thermal units, load demand, and capacity limit of PHES are shown to have a significant impact on the economic performance and wind power accommodation. Quantitative analysis indicates that the presence of PHES in WTHS reduce the negative effects of wind power uncertainty.

Some further studies on the application of this approach in a real world system can be done in future works. The proposed model is formulated for the day-ahead power system operation. Prediction accuracy of wind power increases with the decrease of the prediction timescale. Thus, implementation of multi-timescale scheduling has practical significance and will be considered in future researches.

TABLE 4. Parameters of PHES unit.

g^{max}_{gn}; g^{max}_{pm} (MW)	g^{min}_{gn}; g^{min}_{pm} (MW)	η_{gn}; η_{pm} (m^3/MWh)	$Q^{u}_{max\,p}$; $Q^{u}_{min\,p}$; $Q^{u}_{p,0}$ (10^6 m^3)
90;90	18;18	108;85.2	2.0;0.7224;1.5

APPENDIX

See Figure 13 and Tables 3 and 4.

ACKNOWLEDGMENT

The authors would like to thank Yachao Zhang, Lily Lee, and Xiaobing Liao from the Wuhan University for their helpful discussions. The authors would also like to thank the editor and reviewers for their important suggestions on improving the quality of this paper.

REFERENCES

[1] L. B. Shi, R. Wang, and L. Z. Yao, "Modelling and solutions of coordinated economic dispatch with wind–hydro–thermal complex power source structure," *IET Renew Power Gener.*, vol. 11, no. 3, pp. 262–270, Apr. 2017.

[2] R. Hemmati, "Optimal cogeneration and scheduling of hybrid hydro-thermal-wind-solar system incorporating energy storage systems," *J. Renew. Sustain. Energy*, vol. 10, no. 1, Jan. 2018, Art. no. 014102.

[3] J. J. Chen, Y. B. Zhuang, Y. Z. Li, P. Wang, Y. L. Zhao, and C. S. Zhang, "Risk-aware short term hydro-wind-thermal scheduling using a probability interval optimization model," *Appl. Energy*, vol. 189, pp. 534–554, Mar. 2017.

[4] N. P. Padhy, "Unit commitment—A bibliographical survey," *IEEE Trans. Power Syst.*, vol. 19, no. 2, pp. 1196–1205, May 2004.

[5] T. M. Souza and A. L. Diniz, "An accurate representation of water delay times for cascaded reservoirs in hydro scheduling problems," in *Proc. IEEE Power Eng. Soc. Gen. Meeting*, San Diego, CA, USA, Jul. 2012, pp. 1–7.

[6] G. W. Chang *et al.*, "Experiences with mixed integer linear programming based approaches on short-term hydro scheduling," *IEEE Trans. Power Syst.*, vol. 16, no. 4, pp. 743–749, Nov. 2001.

[7] R. M. Lima, M. G. Marcovecchio, A. Queiroz Novais, and I. E. Grossmann, "On the computational studies of deterministic global optimization of head dependent short-term hydro scheduling," *IEEE Trans. Power Syst.*, vol. 28, no. 4, pp. 4336–4347, Nov. 2013.

[8] J. Jia and X. Guan, "MILP formulation for short-term scheduling of cascaded reservoirs with head effects," in *Proc. 2nd Int. Conf. Artif. Intell. Manage. Sci. Electron. Commerce*, Deng Feng, China, Aug. 2011, pp. 4061–4064.

[9] X.-L. Ge, L.-Z. Zhang, J. Shu, and N.-F. Xu, "Short-term hydropower optimal scheduling considering the optimization of water time delay," *Electr. Power Syst. Res.*, vol. 110, pp. 188–197, May 2014.

[10] A. Borghetti, C. D'Ambrosio, A. Lodi, and S. Martello, "An MILP approach for short-term hydro scheduling and unit commitment with head-dependent reservoir," *IEEE Trans. Power Syst.*, vol. 23, no. 3, pp. 1115–1124, Aug. 2008.

[11] A. J. Conejo, J. M. Arroyo, J. Contreras, and F. A. Villamor, "Self-scheduling of a hydro producer in a pool-based electricity market," *IEEE Trans. Power Syst.*, vol. 17, no. 4, pp. 1265–1272, Nov. 2002.

[12] J. G. Gonzalez and G. A. Castro, "Short-term hydro scheduling with cascaded and head-dependent reservoirs based on mixed-integer linear programming," in *Proc. IEEE Porto Power Tech*, Porto, Portugal, Sep. 2001, pp. 1–6.

[13] J. G. Gonzalez, E. Parrilla, and A. Mateo, "Risk-averse profit-based optimal scheduling of a hydro-chain in the day-ahead electricity market," *Eur. J. Oper. Res.*, vol. 181, no. 3, pp. 1354–1369, Sep. 2007.

[14] X. Guan, A. Svoboda, and C. Li, "Scheduling hydro power systems with restricted operating zones and discharge ramping constraints," *IEEE Trans. Power Syst.*, vol. 14, no. 1, pp. 126–131, Feb. 1999.

[15] Q. Zhai, X. Guan, and F. Gao, "A necessary and sufficient condition for obtaining feasible solution to hydro power scheduling with multiple operating zones," in *Proc. IEEE Power Eng. Soc. Gen. Meeting*, Tampa, FL, USA, Jun. 2007, pp. 1–7.

[16] E. C. Finardi and M. R. Scuzziato, "Hydro unit commitment and loading problem for day-ahead operation planning problem," *Int. J. Elect. Power Energy Syst.*, vol. 44, no. 1, pp. 7–16, 2013.
[17] B. Tong, Q. Zhai, and X. Guan, "An MILP based formulation for short-term hydro generation scheduling with analysis of the linearization effects on solution feasibility," *IEEE Trans. Power Syst.*, vol. 28, no. 4, pp. 3588–3599, Nov. 2013.
[18] L. S. M. Guedes, P. de Mendonça Maia, A. C. Lisboa, D. A. G. Vieira, and R. R. Saldanha, "A unit commitment algorithm and a compact MILP model for short-term hydro-power generation scheduling," *IEEE Trans. Power Syst.*, vol. 32, no. 5, pp. 3381–3390, Sep. 2017.
[19] A. Papavasiliou, S. S. Oren, and B. Rountree, "Applying high performance computing to transmission-constrained stochastic unit commitment for renewable energy integration," *IEEE Trans. Power Syst.*, vol. 30, no. 3, pp. 1109–1120, May 2015.
[20] J. Wang, M. Shahidehpour, and Z. Li, "Security-constrained unit commitment with volatile wind power generation," *IEEE Trans. Power Syst.*, vol. 23, no. 3, pp. 1319–1327, Aug. 2008.
[21] M. Karami, H. A. Shayanfar, J. Aghaei, and A. Ahmadi, "Scenario-based security-constrained hydrothermal coordination with volatile wind power generation," *Renew. Sustain. Energy Rev.*, vol. 28, pp. 726–737, Dec. 2013.
[22] D. Bertsimas and M. Sim, "The price of robustness," *Oper. Res.*, vol. 52, no. 1, pp. 35–53, Jan. 2004.
[23] Y. Wang, Q. Xia, and C. Kang, "Unit commitment with volatile node injections by using interval optimization," *IEEE Trans. Power Syst.*, vol. 26, no. 3, pp. 1705–1713, Aug. 2011.
[24] R. Jiang, J. Wang, M. Zhang, and Y. Guan, "Two-stage minimax regret robust unit commitment," *IEEE Trans. Power Syst.*, vol. 28, no. 3, pp. 2271–2282, Aug. 2013.
[25] B. Hu, L. Wu, and M. Marwali, "On the robust solution to SCUC with load and wind uncertainty correlations," *IEEE Trans. Power Syst.*, vol. 29, no. 6, pp. 2952–2964, Nov. 2014.
[26] D. Bertsimas, E. Litvinov, X. A. Sun, J. Zhao, and T. Zheng, "Adaptive robust optimization for the security constrained unit commitment problem," *IEEE Trans. Power Syst.*, vol. 28, no. 1, pp. 52–63, Feb. 2013.
[27] P. Xiong and P. Jirutitijaroen, "Two-stage adjustable robust optimisation for unit commitment under uncertainty," *IET Gener., Transmiss. Distrib.*, vol. 8, no. 3, pp. 573–582, Mar. 2014.
[28] R. Jiang, M. Zhang, G. Li, and Y. Guan, "Two-stage network constrained robust unit commitment problem," *Eur. J. Oper. Res.*, vol. 234, no. 3, pp. 751–762, May 2014.
[29] B. Hu, L. Wu, X. Guan, F. Gao, and Q. Zhai, "Comparison of variant robust SCUC models for operational security and economics of power systems under uncertainty," *Electr. Power Syst. Res.*, vol. 133, pp. 121–131, Apr. 2016.
[30] C. Wang, F. Liu, S. Mei, F. Qiu, and J. Wang, "Robust unit commitment considering strategic wind generation curtailment," in *Proc. IEEE Power Eng. Soc. Gen. Meeting*, Boston, MA, USA, Jul. 2016, pp. 1–5.
[31] A. Ben-Tal, A. Goryashko, E. Guslitzer, and A. Nemirovski, "Adjustable robust solutions of uncertain linear programs," *Math. Program.*, vol. 99, no. 2, pp. 351–376, 2004.
[32] A. Lorca, X. A. Sun, E. Litvinov, and T. Zheng, "Multistage adaptive robust optimization for the unit commitment problem," *Oper. Res.*, vol. 64, no. 1, pp. 32–51, Feb. 2016.
[33] M. Zugno, J. M. Morales, and H. Madsen, "Commitment and dispatch of heat and power units via affinely adjustable robust optimization," *Comput. Oper. Res.*, vol. 75, pp. 191–201, Nov. 2016.
[34] C. Lee, C. Liu, S. Mehrotra, and M. Shahidehpour, "Modeling transmission line constraints in two-stage robust unit commitment problem," *IEEE Trans. Power Syst.*, vol. 29, no. 3, pp. 1221–1231, May 2014.
[35] M. S. Guney and Y. Tepe, "Classification and assessment of energy storage systems," *Renew. Sustain. Energy Rev.*, vol. 75, pp. 1187–1197, Aug. 2017.
[36] S. Mahdavi, R. Hemmati, and M. A. Jirdehi, "Two-level planning for coordination of energy storage systems and wind-solar-diesel units in active distribution networks," *Energy*, vol. 151, pp. 954–965, May 2018.
[37] R. Hemmati, S. M. S. Ghiasi, and A. Entezariharsini, "Power fluctuation smoothing and loss reduction in grid integrated with thermal-wind-solar-storage units," *Energy*, vol. 152, pp. 759–769, Jun. 2018.
[38] J. P. Deane, B. P. Ó. Gallachóir, and E. J. McKeogh, "Techno-economic review of existing and new pumped hydro energy storage plant," *Renew. Sustain. Energy Rev.*, vol. 14, no. 4, pp. 1293–1302, 2010.
[39] A. M. Foley, P. G. Leahy, K. Li, E. J. Mckeogh, and A. P. Morrison, "A long-term analysis of pumped hydro storage to firm wind power," *Appl. Energ.*, vol. 137, pp. 638–648, Jan. 2015.
[40] J. I. Pérez-Díaz and J. Jiménez, "Contribution of a pumped-storage hydropower plant to reduce the scheduling costs of an isolated power system with high wind power penetration," *Energy*, vol. 109, pp. 92–104, Aug. 2016.
[41] K. Bruninx, Y. Dvorkin, E. Delarue, H. Pandžić, W. D'haeseleer, and D. S. Kirschen, "Coupling pumped hydro energy storage with unit commitment," *IEEE Trans. Sustain. Energy*, vol. 7, no. 2, pp. 786–796, Apr. 2016.
[42] Z. Ming, Z. Kun, and W. Liang, "Study on unit commitment problem considering wind power and pumped hydro energy storage," *Int. J. Elect. Power Energy Syst.*, vol. 63, pp. 91–99, Dec. 2014.
[43] M. E. Khodayar, M. Shahidehpour, and L. Wu, "Enhancing the dispatchability of variable wind generation by coordination with pumped-storage hydro units in stochastic power systems," *IEEE Trans. Power Syst.*, vol. 28, no. 3, pp. 2808–2818, Aug. 2013.
[44] W. Wang, C. Li, X. Liao, and H. Qin, "Study on unit commitment problem considering pumped storage and renewable energy via a novel binary artificial sheep algorithm," *Appl. Energy*, vol. 187, pp. 612–626, Feb. 2017.
[45] R. Jiang, J. Wang, and Y. Guan, "Robust unit commitment with wind power and pumped storage hydro," *IEEE Trans. Power Syst.*, vol. 27, no. 2, pp. 800–810, May 2012.
[46] M. S. Al-Swaiti, A. T. Al-Awami, and M. W. Khalid, "Co-optimized trading of wind-thermal-pumped storage system in energy and regulation markets," *Energy*, vol. 138, pp. 991–1005, Nov. 2017.
[47] A. Shukla and S. Singh, "Clustering based unit commitment with wind power uncertainty," *Energy Convers. Manage.*, vol. 111, pp. 89–102, Mar. 2016.
[48] Q. Wang, X. J. Luo, N. W. Gong, and H. L. Ma, "Day-ahead optimal dispatching of wind-solar-hydro-thermal combined power system with pumped-storage hydropower integration," in *Proc. IEEE Innov. Smart Grid Technol. Asia*, Singapore, May 2018, pp. 430–434.
[49] M. A. Igder, T. Niknam, and M. H. Khooban, "Bidding strategies of the joint wind, hydro, and pumped-storage in generation company using novel improved clonal selection optimisation algorithm," *IET Sci. Meas. Technol.*, vol. 11, no. 8, pp. 991–1001, 2017.
[50] X. B. Wang, J. X. Chang, X. J. Meng, and Y. M. Wang, "Short-term hydro-thermal-wind-photovoltaic complementary operation of interconnected power systems," *Appl. Energ.*, vol. 229, pp. 945–962, Nov. 2018.
[51] A. J. Wood and B. F. Wollenberg, *Power Generation, Operation, and Control*, 2nd ed. New York, NY, USA: Wiley, 1996.
[52] E. C. Finardi and E. L. Da Silva, "Solving the hydro unit commitment problem via dual decomposition and sequential quadratic programming," *IEEE Trans. Power Syst.*, vol. 21, no. 2, pp. 835–844, May 2006.
[53] E. C. Finardi and E. L. da Silva, "Unit commitment of single hydroelectric plant," *Electr. Power Syst. Res.*, vol. 75, pp. 116–123, Aug. 2005.
[54] H. B. Sun and B. M. Zhang, "A systematic analytical method for quasi-steady-state sensitivity," *Electr. Power Syst. Res.*, vol. 63, no. 2, pp. 141–147, Sep. 2002.
[55] M. Carrión and J. M. Arroyo, "A computationally efficient mixed-integer linear formulation for the thermal unit commitment problem," *IEEE Trans. Power Syst.*, vol. 21, no. 3, pp. 1371–1378, Aug. 2006.
[56] S. P. Bradley, A. C. Hax, and T. L. Magnanti, *Applied Mathematical Programming*. Reading, MA, USA: Addison-Wesley, 1977.
[57] D. A. Babayev, "Piece-wise linear approximation of functions of two variables," *J. Heuristics*, vol. 2, no. 4, pp. 313–320, 1997.
[58] A. L. Soyster, "Convex programming with set-inclusive constraints and applications to inexact linear programming," *Oper. Res.*, vol. 21, no. 5, pp. 1154–1157, Sep. 1973.
[59] M. Yang, M. Q. Wang, F. L. Cheng, and W. J. Lee, "Robust economic dispatch considering automatic generation control with affine recourse process," *Int. J. Elect. Power Energy Syst.*, vol. 81, pp. 289–298, Oct. 2016.
[60] R. W. Ferrero, S. M. Shahidehpour, and V. C. Ramesh, "Transaction analysis in deregulated power systems using game theory," *IEEE Trans. Power Syst.*, vol. 12, no. 3, pp. 1340–1347, Aug. 1997.
[61] EirGrid. *EirGrid System Performance Data*. Accessed: Sep. 2018. [Online]. Available: http://www.eirgrid.com/operations/systemperformancedata
[62] X.-Y. Ma, Y.-Z. Sun, and H.-L. Fang, "Scenario generation of wind power based on statistical uncertainty and variability," *IEEE Trans. Sustain. Energy*, vol. 4, no. 4, pp. 894–904, Oct. 2013.
[63] *IEEE 118-Bus System Data*. Accessed: Oct. 2018. [Online]. Available: http://motor.ece.iit.edu/data/JEAS_IEEE118.doc

[64] R. D. Zimmerman, C. E. Murillo-Sánchez, and R. J. Thomas, "MATPOWER: Steady-state operations, planning, and analysis tools for power systems research and education," *IEEE Trans. Power Syst.*, vol. 26, no. 1, pp. 12–19, Feb. 2011.
[65] *Gurobi Optimizer Reference Manual*, Gurobi Optim., Houston, TX, USA, 2018.
[66] C. Peng, P. Xie, L. Pan, and R. Yu, "Flexible robust optimization dispatch for hybrid wind/photovoltaic/hydro/thermal power system," *IEEE Trans. Smart Grid*, vol. 7, no. 2, pp. 751–762, Mar. 2016.

PEI XIA received the B.S. and M.S. degrees in electrical engineering from China Three Gorges University, Yichang, China, in 2009 and 2012, respectively. She is currently pursuing the Ph.D. degree in electrical engineering with Wuhan University, Wuhan, China. Her research interest includes the optimal scheduling of power systems with renewable energy.

CHANGHONG DENG received the Ph.D. degree from the School of Electrical Engineering, Wuhan University, Wuhan, China, in 2007, where she is currently a Professor. Her research interests include power system security and stability analysis, optimal control theory, and renewable energy integration.

YAHONG CHEN received the B.S. degree in electrical engineering and automation from Guizhou University, in 2013, and the M.S. degree in electrical engineering from the Harbin Institute of Technology Shenzhen Graduate School, Shenzhen, in 2016, respectively. He is currently pursuing the Ph.D. degree with Wuhan University, Wuhan, China. His research interests include the microgrids operation, energy management, power systems economic dispatch, and sea water pumped storage system operation.

WEIWEI YAO received the B.S. and M.S. degrees in electrical engineering from China Three Gorges University, China, in 2010 and 2014. He is currently pursuing the Ph.D. degree with Wuhan University, China. His research interests include micro grids operation and seawater pumped storage system operation.